Vertically aligned carbon nanofibers as sacrificial templates for nanofluidic structures

A. V. Melechko,[a),b)] T. E. McKnight, M. A. Guillorn,[c)] and V. I. Merkulov
Molecular-Scale Engineering and Nanoscale Technologies Research Group, Oak Ridge National Laboratory, Oak Ridge, Tennessee 37831

B. Ilic
School of Applied and Engineering Physics, Cornell University, Ithaca, New York 14853

M. J. Doktycz
Life Sciences Division, Oak Ridge National Laboratory, Oak Ridge, Tennessee 37831

D. H. Lowndes
Condensed Matter Sciences Division, Oak Ridge National Laboratory, Oak Ridge, Tennessee 37831

M. L. Simpson[b),c)]
Molecular-Scale Engineering and Nanoscale Technologies Research Group, Oak Ridge National Laboratory, Oak Ridge, Tennessee 37831

(Received 1 August 2002; accepted 16 December 2002)

We report a method to fabricate nanoscale pipes (''nanopipes'') suitable for fluidic transport. Vertically aligned carbon nanofibers grown by plasma-enhanced chemical vapor deposition are used as sacrificial templates for nanopipes with internal diameters as small as 30 nm and lengths up to several micrometers that are oriented perpendicular to the substrate. This method provides a high level of control over the nanopipe location, number, length, and diameter, permitting them to be deterministically positioned on a substrate and arranged into arrays. © *2003 American Institute of Physics.* [DOI: 10.1063/1.1544058]

The fabrication of devices that function on the nanometer scale requires new approaches when standard microfabrication techniques cannot be scaled down. One such approach, the use of the materials such as carbon nanotubes and carbon nanofibers that self-assemble into nanostructures, has been successfully applied in nanoelectronics.[1,2] Vertically aligned carbon nanofibers (VACNFs) that can be synthesized highly deterministically,[3–6] have been utilized in a variety of nanodevices, such as VACNF-based electrochemical probes designed for intracellular characterization[7] or gated cathode field-emitters.[8] Another nanofabrication approach that has been proposed for construction of nanofluidic devices is to use templates made of sacrificial materials defined by electron-beam lithography (EBL).[9]

In the work reported here, we combine these two approaches to demonstrate the use of carbon nanofibers as self-assembled sacrificial templates for the synthesis of nanopipes, which are extended hollow structures that can be as long as a few micrometers, with internal diameters as small as 30 nm. Such nanopipes can be implemented as functional elements in gas- and liquid-phase fluidic devices. Several applications of nanopipes can be envisioned, including high-throughput sensing, analysis of molecular species,[10] and fluidic interfaces to live cells. Compared to conventional pulled micropipettes,[11] which are single-element probing devices, the fabrication of nanopipes can be integrated in a parallel manner into microchip fabrication and lab-on-a-chip devices. Nanopipe-based devices may be used as nanoporous membranes[12–14] for molecular control, as they can be synthesized with very good control of the nanopore geometry. The ability to define the nanopipe location, number (e.g., array or single), length and internal diameter is mainly provided by the ability to deterministically grow vertically aligned carbon nanofibers.[3]

The nanopipe fabrication process is depicted in Fig. 1. Thin (80-nm), low-stress Si_3N_4 membranes were used as a substrate so that the access holes to the nanopipes could be opened from the back side of the chip[9] [Fig. 1(a)]. EBL was used to define catalyst sites for deterministic growth of VACNFs [Fig. 1(b)]. The nanofibers were grown [Fig. 1(c)] in a glow discharge dc plasma consisting of an ammonia/acetylene gas mixture at 700 °C.[3] A scanning electron microscope (SEM) image of the resultant array of fibers is shown in Fig. 2. In the next step [Fig. 1(d)], the nanopipe walls were formed by coating the nanofibers and chip surface with a 100-nm-thick layer of SiO_2 using a silane-based, plasma-enhanced chemical vapor deposition process. Resist was then spun-on and the tips of the nanopipes were opened by reactive-ion etching. The Ni particle was removed in nitric acid, providing access to the carbon nanofiber [Figs. 1(e), 1(f), and 1(g)], that successively were etched from the nanopipe interior in an oxygen plasma [Fig. 1(h)]. Finally, openings through the silicon nitride membrane were produced by exposing the chip to SF_6/O_2-based reactive ion etching, with the newly formed nanopipes serving as a mask, thereby

[a)]Also with: Department of Electrical and Computer Engineering, University of Tennessee, Knoxville, TN 37996; electronic mail: meleshkoav@ornl.gov
[b)]Also with: Center for Environmental Biotechnology, University of Tennessee, Knoxville, TN 37996.
[c)]Also with: Materials Science and Engineering Department, University of Tennessee, Knoxville, TN 37996.

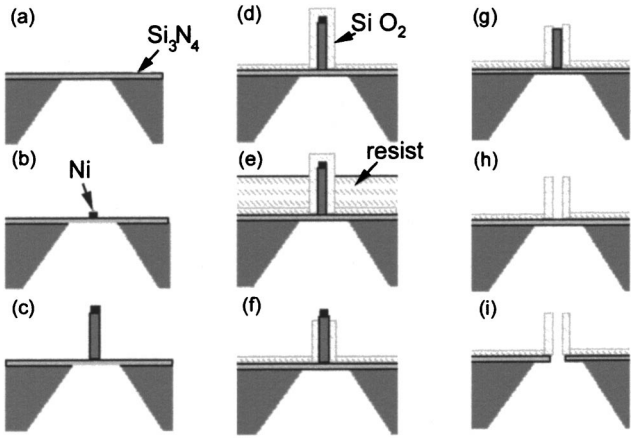

FIG. 1. Steps for fabrication of nanopipes on a thin membrane. (a) Si_3N_4 membrane on Si substrate with back-side-etched window; (b) Ni particles are defined via EBL and lift-off techniques; (c) VACNFs are grown by plasma-enhanced chemical vapor deposition; (d) the VACNFs and substrate are coated with SiO_2; (e) resist is spun on; (f) SiO_2 is removed from the tips by reactive-ion etching and the remaining resist is removed; (g) the Ni particle is removed in an HNO_3 wet etch; (h) the carbon nanofiber is etched away in an O_2 plasma; (i) the Si_3N_4 membrane is etched from the front side, through the nanopipes, by reactive-ion etching.

assuring self-alignment of the back-side holes with the nanopipes [Fig. 1(i)]. The SEM images of the final structure are presented in Fig. 3. To produce the structures presented in this letter, the catalyst dot size was larger than 400 nm in diameter due to the limitations of the EBL tool used, thus multiple fibers (2–3) were produced on each dot [Fig. 2].[3]

The functionality of nanopipes has been demonstrated by observing fluidic transport between two fluid regions that were physically separated by a membrane containing the nanopipe pores. To observe fluid transport, we exploited the fluorogenic property of propidium iodide, a nucleic acid stain that is fluorescently enhanced by a factor of 20–30 upon its intercalation between the bases of double-stranded DNA. By placing a solution of this dye on one side of the nanopipe

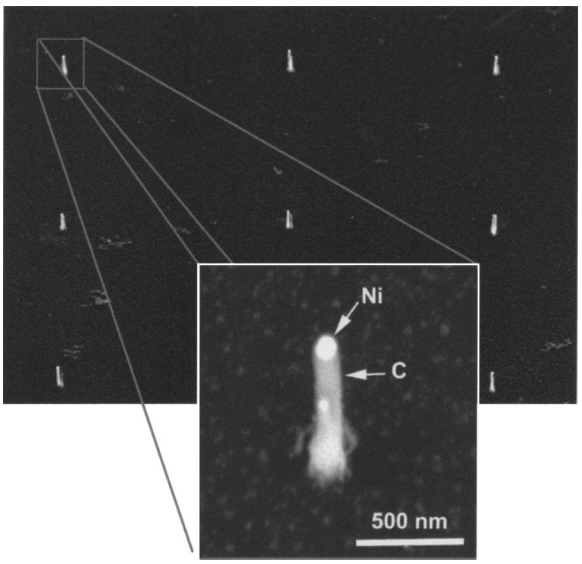

FIG. 2. Scanning electron micrograph of an array of VACNFs grown on top of a Si_3N_4 membrane (30° view, 10-μm spacing, 1-μm average height, 100-nm diameter). The evaporated Ni catalyst dots were sufficiently large that most of them separated into two distinct nanoparticles during sintering at 700 °C, so that two VACNFs were grown at most locations.

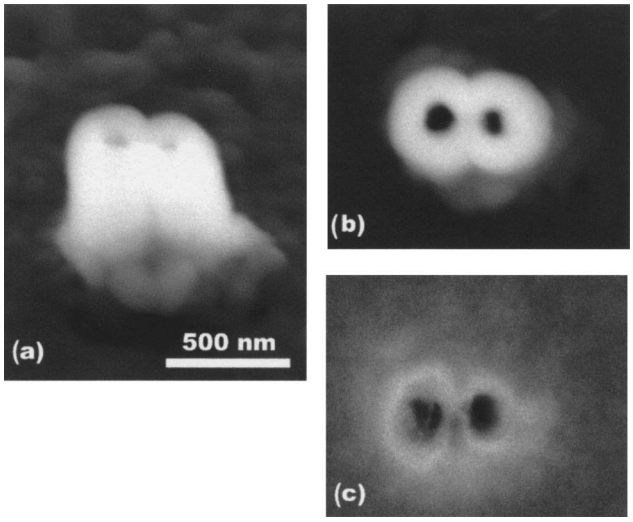

FIG. 3. SEM images of the final nanopipe structures: (a) side view at 30°; (b) top view (nanopipe side); (c) bottom view (Si_3N_4 membrane side). Note that each of the two nanopipes acts faithfully as a mask during the etching-through step.

membrane, and a solution of double-stranded DNA on the opposing side, the transport of material through the pipe could be observed by an enhanced fluorescent response in the regions where the fluids mixed. To enable visualization of this interaction using fluorescence microscopy, a fixture was fabricated that elevated the nanopipe membrane approximately 1 mm above the surface of a glass microscope slide. Approximately 10 μl of the two solutions [6-μM propidium iodide and 0.5-μg/μl plasmid DNA (pgreenlantern-1)] was then placed on the top (propidium iodide) and bottom (DNA) surfaces of the membrane, respectively. Prior to loading, the dry nanopipe array was imaged in transmission mode using white light illumination [Fig. 4(a)]. After loading, the diffusive transport of material between the two solutions was observed using two-dimensional images acquired with an optical microscope with an epifluorescence attachment, a cooled CCD camera, and a TRITC filter set (545-nm excitation/620-nm emission). Immediately upon loading, plumes of fluorescence could be observed in the DNA solution at some of the nanopipe positions as propidium iodide diffused through the nanopipes and intercalated into the plasmid DNA [Figs. 4(b) and 4(c)]. After a few minutes, these plumes tended to decrease and stop [Fig. 4(d)], possibly due to the large structure of the plasmid tending to diffuse into and clog the nanoscale pipe pores. Over time, the fluorescence at the pipe positions was noted to increase, perhaps indicative of the presence of increasing amounts of propidium-iodide-stained DNA within the nanopipe.

Following demonstration of diffusive transport between the propidium iodide and DNA solutions, the fixture was modified to enable electrical connection to the fluid droplets on either side of the nanopipe membrane. Voltages were applied between the two solutions, with the positive electrode in the propidium iodide solution and the negative electrode in the DNA solution. Under these conditions, there will be electrophoretic mobility of the propidium ion (positively charged) towards the negative electrode in the DNA solution, as well as DNA (negatively charged phosphate backbone) migration to the positive electrode in the propidium iodide

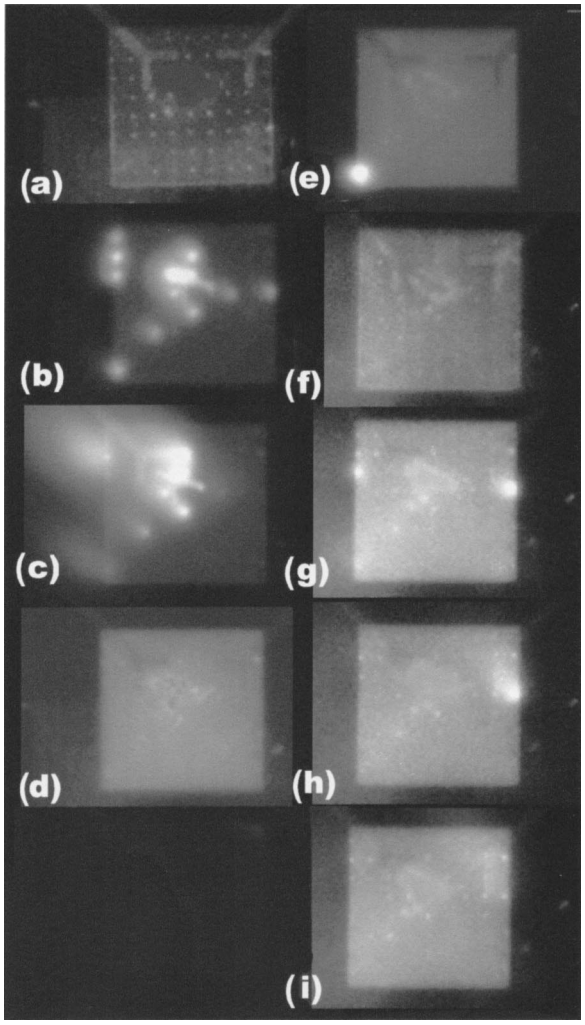

FIG. 4. Observation of fluidic transport through nanopipe membranes by diffusive mixing and electrokinetic interaction of two membrane-isolated solutions (propidium iodide and DNA). Upon interaction, the propidium iodide fluorescence increases dramatically as it intercalates with the DNA. (a) A dry array of nanopipes viewed in white light illumination; (b) and (c) fluorescence images taken 1 and 3 min after application of propidium iodide and DNA solutions, respectively; (d) fluorescent plumes subsided and uniform fluorescent background was observed; (e) after washing in deionized water and rewetting with propidium iodide and DNA (the plume appeared from the nanopipe displayed in Fig. 3); (f) the plume is subsided after 3 min; (g) and (h) fluorescence images taken 1 and 3 min after 5 V was applied to the solution between opposite sides of the membrane, respectively; (i) the plumes stopped after 5 min.

solution. Further, as the nanopipe is composed of silica, the negative surface charges on the silica will support electroosmotic flow (see for example, Ref. 15) due to cation stacking and their subsequent migration towards the negative electrode in the DNA solution. The fixture was mounted on the fluorescent microscope platform and solutions were applied as previously described. Following initial plume formation due to diffusive transport [Fig. 4(e)], the plumes dispersed, and no additional plume formation was observed [Fig. 4(f)]. Application of a 5-V potential between the two fluids resulted in the sudden generation of a large plume from a few nanopipes [Figs. 4(g) and 4(h)] that subsided after about 5 min [Fig. 4(i)]. Both the diffusive and electrokinetically-induced plume generation could be reproduced after thorough rinsing of the device in nanopure water.

In summary, a concept of nanofabrication based upon the synthesis of sacrificial self-assembled nanostructures (VACNFs) grown at predetermined locations as templates for the formation of nanopipe structures has been demonstrated. The functionality of nanopipes for diffusive and electrokinetic transport of small molecules has been confirmed.

We would like to thank P. Fleming for help with sample preparation. This research was supported by the Laboratory Directed Research and Development Program of Oak Ridge National Laboratory (ORNL), by the Office of Basic Energy Sciences, Division of Materials Sciences, U.S. Department of Energy, and by the Defense Advanced Research Projects Agency under Contract No. 1868HH26X1 with ORNL. The research was carried out at ORNL, managed by UT-Battelle, LLC, for the U.S. Department of Energy under Contract No. DE-AC05-00OR22725, and in part at the Cornell Nanofabrication Facility (a member of the National Nanofabrication Users Network) which is supported by the National Science Foundation under Grant ECS-9731293, its users, Cornell University, and Industrial Affiliates.

[1] Y. Huang, X. F. Duan, Y. Cui, L. J. Lauhon, K. H. Kim, and C. M. Lieber, Science **294**, 1313 (2001).
[2] A. Bachtold, P. Hadley, T. Nakanishi, and C. Dekker, Science **294**, 1317 (2001).
[3] V. I. Merkulov, D. H. Lowndes, Y. Y. Wei, G. Eres, and E. Voelkl, Appl. Phys. Lett. **76**, 3555 (2000).
[4] Z. F. Ren, Z. P. Huang, J. W. Xu, J. H. Wang, P. Bush, M. P. Siegal, and P. N. Provencio, Science **282**, 1105 (1998).
[5] L. Delzeit, C. V. Nguyen, R. M. Stevens, J. Han, and M. Meyyappan, Nanotechnology **13**, 280 (2002).
[6] M. Chhowalla, K. B. K. Teo, C. Ducati, N. L. Rupesinghe, G. A. J. Amaratunga, A. C. Ferrari, D. Roy, J. Robertson, and W. I. Milne, J. Appl. Phys. **90**, 5308 (2001).
[7] M. A. Guillorn, T. E. McKnight, A. Melechko, V. I. Merkulov, P. F. Britt, D. W. Austin, D. H. Lowndes, and M. L. Simpson, J. Appl. Phys. **91**, 3824 (2002).
[8] M. A. Guillorn, A. V. Melechko, V. I. Merkulov, E. D. Ellis, C. L. Britton, M. L. Simpson, D. H. Lowndes, and L. R. Baylor, Appl. Phys. Lett. **79**, 3506 (2001).
[9] C. K. Harnett, G. W. Coates, and H. G. Craighead, J. Vac. Sci. Technol. B **19**, 2842 (2001).
[10] J. Li, D. Stein, C. McMullan, D. Branton, M. J. Aziz, and J. A. Golovchenko, Nature (London) **412**, 166 (2001).
[11] T. Vo-Dinh, B. Cullum, and G. D. Griffin, Radiation Research **156**, 437 (2001).
[12] C. R. Martin, Science **266**, 1961 (1994).
[13] S. A. Miller, V. Y. Young, and C. R. Martin, J. Am. Chem. Soc. **123**, 12335 (2001).
[14] L. Sun and R. M. Crooks, J. Am. Chem. Soc. **122**, 12340 (2000).
[15] S. L. Zeng, C. H. Chen, J. C. Mikkelsen, and J. G. Santiago, Sens. Actuators B **79**, 107 (2001).